

# An Application of Quantitative Geomorphometric Indicators in identifying 'Susceptible Zones by Using SVM Model (Case study: Khorramabad- Pol Zal Freeway)

Ali Ahmadabadi

Kharazmi University

Mitra Saberi (✉ [msaberi.khu@gmail.com](mailto:msaberi.khu@gmail.com))

Kharazmi University <https://orcid.org/0000-0002-5841-2783>

---

## Research

**Keywords:** Quantitative Geomorphometric, SVM Model, Pol Zal Freeway

**Posted Date:** January 29th, 2021

**DOI:** <https://doi.org/10.21203/rs.3.rs-154476/v1>

**License:** © ⓘ This work is licensed under a Creative Commons Attribution 4.0 International License.

[Read Full License](#)

---

1  
2  
3  
4 **An Application of Quantitative**  
5 **Geomorphometric Indicators in identifying**  
6 **‘[Susceptible Zones by Using SVM Model (Case**  
7 **study: Khorramabad- Pol Zal Freeway)**

8  
9  
10  
11 Ali Ahmadabadi<sup>1</sup> , Mitra Saberi<sup>2</sup>  
12  
13

14  
15  
16 **Abstract**  
17

18 Geomorphometry is the quantitative measurement of landforms based on height changes influenced by distance  
19 function. Geomorphometry indices express the characteristics of the terrain quantitatively. The present study  
20 emphasizes the use of geo-morphometric parameters and SVM algorithm to identify areas prone to landslide in  
21 Khorramabad- Paul Zal freeway as one of the important roads in the country. Other indices include slope,  
22 aspect, lithology, fault condition, drainage and land use which are applied together with the geometric indices  
23 such as profile curvature, plan curvature and total curvature use, artificial intelligence approach and linear  
24 functions and polynomial SVM algorithm to identify areas prone to landslides. The results show using  
25 Geomorphometric indices play an important role in increasing accuracy of assessing and identifying areas with  
26 an increasing the risk of landslides and assessing the accuracy through using land survey data shows that  
27 polynomial functions are more accurate in identifying areas prone to landslides than SVM algorithm linear  
28 function.  
29

---

<sup>1</sup>. Assistant prof. in Geomorphology, Kharazmi University, ahmadabadi@khu.ac.ir.

<sup>2</sup>. PhD of Geomorphology, Kharazmi University ,msaberi.khu@gmail.com.

## 32 Introduction

33 Landslide has a negative effect on human life and  
 34 economic activities all over the world  
 35 (Pourghasemi et al., 2012, Nadim et al., 2006).  
 36 According to 2012 World Disaster Report (2011-  
 37 2002) landslide is among the world's seven natural  
 38 disasters (IFRCRCS., 2012). Several methods have  
 39 been proposed to evaluate the landslide  
 40 susceptibility map that can be divided into two  
 41 broad classification categories: qualitative  
 42 (subjective) and quantitative (objective) (Fell et al.,  
 43 2008). However, Landslides are usually complex  
 44 systems and to predict the sensitivity of their  
 45 occurrence there needs to be different  
 46 geomorphologic, geologic, hydrological, land cover  
 47 and other data on environmental factors (Ling Peng  
 48 et al., 2014). There are no specific universal  
 49 guidelines for the selection of the factors affecting  
 50 global mapping of landslide susceptibility (Yalcin.,  
 51 2008). Previous studies were usually willing to  
 52 provide little information or a model with low  
 53 quality performance (Guzzetti et al., 2006; Frattini  
 54 et al., 2010) which were not satisfactory for final  
 55 users and there were limitations associated with  
 56 these studies) Chung and Fabbri., 2003). This is the  
 57 necessity because of which methods with better  
 58 criteria for identifying significant environmental  
 59 factors leading to landslide in line with the  
 60 environmental planning are needed. With regard to  
 61 improved methods of data analysis and technical  
 62 and artistic techniques such as of Artificial Neural  
 63 Networks (Lee et al., 2004; Yesilnacar and Topal.,  
 64 2005; Nefeslioglu et al., 2008), fuzzy logic  
 65 (Ercanoglu and Gokceoglu., 2004; Pradhan et al.,  
 66 2009; Akgun et al., 2012), neural - fuzzy, (Oh and  
 67 Pradhan, 2011; Bui et al., 2012) Decision tree  
 68 (Saito et al., 2009; Wan., 2009; Nefeslioglu et al.,  
 69 2010; Yeon et al., 2010) algorithm and support  
 70 Mashyn-Brdar Yao et al., 2008; Yilmaz., 2009;  
 71 Marjanovi'c et al., 2011; Pradhan., 2013) The  
 72 researchers were able to use these techniques for  
 73 mapping the landslide. Yamani et al (2013) in a  
 74 study in Darakeh basin, performed the landslide  
 75 zoning using four functions of SVM algorithm. The  
 76 results showed that through identifying areas prone  
 77 to landslide, the external function of this algorithm  
 78 best matches the reality. In another study, Chan Su  
 79 and et al (2012) examined the ability of the SVM  
 80 model in landslides caused by earthquakes using  
 81 GIS software in China's Jianjiang Basin. The  
 82 results suggest more appropriate radial function  
 83 SVM algorithm in comparison to other functions,  
 84 in predicting of landslides. A review of the  
 85 literature in this area suggests few studies have  
 86 been done on the involvement of the scope and  
 87 impact geomorphometric indicators. Among such  
 88 limited studies, one can mention the research

89 Talebi and et al (2008) have done; He combined  
 90 three longitudinal profiles (concave, flat and  
 91 convex) and three types of plans (convergent,  
 92 parallel and divergent) to provide the domain  
 93 model for slope stability of the composition. In this  
 94 model, the impact of the plans and profiles was  
 95 investigated in unstable slopes and landslides.  
 96 According to the results, it can be said that the  
 97 slope of the convex and concave divergent and  
 98 convergent are generally more stable than the steep,  
 99 smooth slope, while the other two are located on  
 100 the intermediate level. So far, there have been no  
 101 comprehensive studies of landslide susceptibility  
 102 assessment in the study area.

103 Furthermore, the limited information about the  
 104 area, has not let us do a survey to assess the exact  
 105 number of potential landslides. landslides occurred  
 106 on Khorramabad - Pol Zal highway in south west  
 107 of Iran (Figure 1) and near the historic landslide  
 108 Simereh which is a serious threat to social and  
 109 economic stability of the region; As a result of the  
 110 construction of the main road which connects the  
 111 central and western regions of Iran Khuzestan plain  
 112 and the Persian Gulf, new trenches in susceptible  
 113 geological formations, has increased the probability  
 114 of potential landslides and slope instability, which  
 115 has become a serious and inevitable problem  
 116 (Yamani et al., 2014). That's why the prediction of  
 117 landslides so as to prevent new landslide, new slips  
 118 and also activation of older landslides, it is  
 119 essential to reduce the risk of the zone. The purpose  
 120 of this study is to evaluate SVM method to identify  
 121 landslide prone zones with emphasis on the use of  
 122 Geomorphometric parameters.

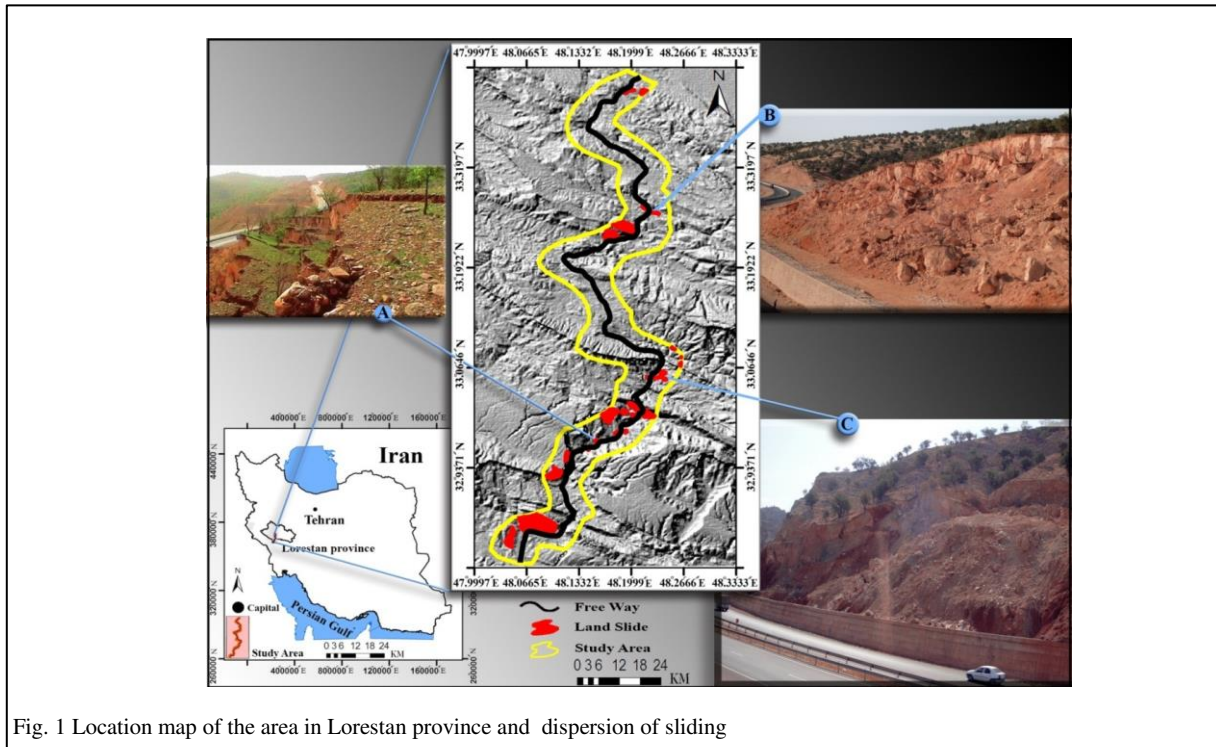
## 123 Extent of the study

124 The newly built Khorramabad - Paul Zal highway  
 125 with a length of 104 km, connects the city of  
 126 Khorramabad to Andimeshk. Beginning of the path  
 127 has of latitude 33 26' Northern and a longitude of  
 128 48 12 East is the direction of latitude 32 48 5  
 129 Northern and longitude 48 04 Eastern passes. This  
 130 ranges from the northwest to the southeast of the  
 131 Zagros Folded Belt and is part of the  
 132 Himalayan Alps Upper Cretaceous platform that  
 133 converges the Arabian and Eurasian there (Talbot  
 134 & Alavi., 1996). The aforementioned path with an  
 135 area of 480/968 KM<sup>2</sup>; is like a strip of variable  
 136 width from 5 to 7 km that has been chosen based  
 137 on the occurrence of landslides and their impact  
 138 that can be dominant on the road slopes. The roads  
 139 are often built in the mountains and at the  
 140 confluence of the valleys, and they pass over  
 141 embankments or bridges. The starting point of the

142 road is located in Zagros mountains folding along  
 143 Zagros mountains which passes the approximate  
 144 direction of North - South, at the height of 1200  
 145 meters, the middle points of the road, with a height  
 146 of 2315 meters are located in the mountain and the  
 147 road ends up at the height of 320 meters. According  
 148 the relatively large difference in height, the area has  
 149 several different climates. Therefore, based on  
 150 Domarten four-staged climate classification there  
 151 will be humid, sub-humid, Mediterranean and

152 semi-arid (Yamani et al., 2014). The average  
 153 annual rainfall is between 322-578 mm which  
 154 varies from north to south. Geomorphological  
 155 construction of the region can be divided into  
 156 Northern and Southern areas by thrust fault Rit-  
 157 Sultan. Differences in the extent and severity of  
 158 folds and faults in tectonic result is of significant  
 159 difference in both North and South Northern  
 160 regions.

161



162

163

164

165 **Data and Methods**

166 In this research, three topographic maps of  
 167 Khorramabad, Bydrubeh and Khalil Akbar with a  
 168 scale of 1: 50,000 and two oil-company geological  
 169 maps of Khorramabad and balarood with a scale of  
 170 1: 100,000 and 90 m SRTM DEM have formed the  
 171 basic. Landsat TM images were used for the  
 172 preparation of land use and IRS pictures (PAN) by  
 173 the numbers (A48/66), (C47/66) Related to 2003  
 174 and 2005 to identify landslides before road  
 175 construction. In addition, to complete landslide  
 176 layer in inventory field work through using a GPS  
 177 device height and the position of new landslides  
 178 after construction operations on land, were  
 179 registered on the ground matched with topographic  
 180 maps and satellite images. Also geomorphometric  
 181 indices were calculated by analyzing an equation in  
 182 LANDSERF geomorphometric software and the  
 183 output was found in raster format in ArcGIS  
 184 environment.

185 **SVM algorithm**

186

187

188

189

190

191

192

193

194

195

196

197

198

199

200

201

202

203

204

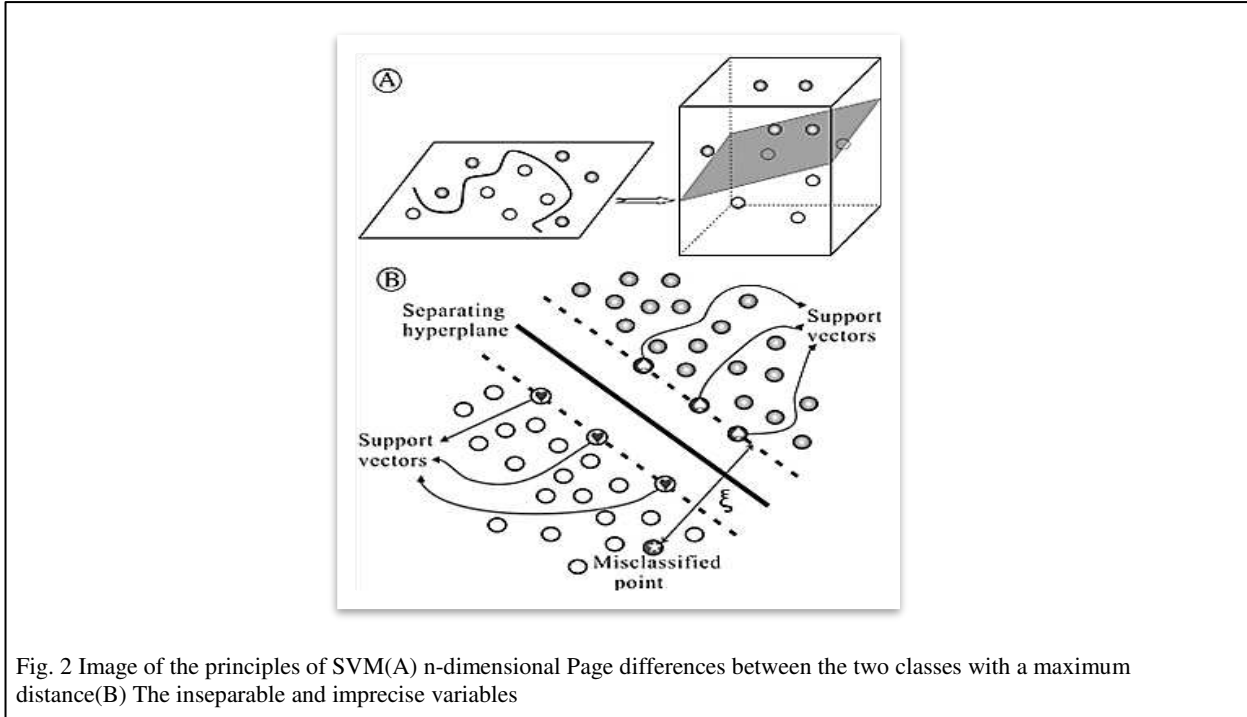
205

206

207

208

SVM cognitive algorithms are used to evaluate  
 and test a series of data (Yao et al., 2008). In  
 recent years, the algorithm has grabbed much  
 attention due to good performance in  
 classifying and improved fault tolerance. SVM  
 is actually a technique based on random  
 sampling that can reduce cognitive complexity  
 problem by maintaining the original  
 information. Support vector machine (SVM)  
 Algorithm was presented by Vapnik in 1995,  
 based on statistical learning theory and  
 dimensional theory and includes a training  
 phase bound with the input and output goals.  
 According to the statistical learning theory,  
 Machine learning error rate for unclassified  
 data can be considered as the extended error  
 rate. These bounds are functions of the overall  
 cognitive error rate and show the extent of  
 complexity of the classifiers (Yamani et al.,  
 2013). In order to minimize extended error  
 rates training error rate and classifier's  
 complexity, should be reduced. This can be  
 done with maximizing separation margin.



210

211 Fig. 2 Image of the principles of SVM(A) n-dimensional Page differences between the two classes with a maximum  
 212 distance(B) The inseparable and imprecise variables

213

$$236 \quad \lambda_i (y_i ((w \cdot x_i) + b)) \geq 1 - \xi_i.$$

214 Details of the two-class SVM modeling is  
 215 summarized as follows (Yao et al., 2008):

237

$$L = \frac{1}{2} \|W\|^2 - \frac{1}{vn} \sum_{i=1}^n \xi_i$$

216 Given a set of distinct cell line

238

$$217 \quad fX_i(i = 1, 2, \dots, n)$$

218 Cells which include two classes as  $y_i = \pm 1$   
 219 Marked. The purpose of SVM model is to Find a  
 220 distinction between two classes -N size, which is  
 221 determined by the maximum gap. Mathematically,  
 222 this concept can be taken with these words:

239 **Geomorphometric indicators of the range**

$$223 \quad \frac{1}{2} \|W\|^2$$

224 Which is subject to the following restrictions:

240 Geomorphometric characteristics express the shape  
 241 of ranges which are prone to slip quantitatively.  
 242 Using values obtained from the DEM products  
 243 such as slope, profile curvature, plan curvature,  
 244 width curvature, and the general curvature of range  
 245 morphometric characteristics of landforms  
 246 (landslide) (Fisher et al., 2004; Pike., 2000;  
 247 Wood1996). Convexity and concavity and second  
 248 derivatives with respect to the levels that are  
 249 generally known under the name of curvature and  
 250 curvature can be used to measure the roughness of  
 251 the surface. The amount of curvature in different  
 252 types in the raster digital elevation model is  
 253 calculated pixel by pixel and for each cell of a  
 254 fourth degree polynomial equation is used  
 255 (Relationship between 1, 2 and 3). In a window  
 256 with dimensions of 3 x 3 is calculated (Figure 3).  
 257 Since the curvature has been calculated using a  
 258 moving window of eight neighboring cells it is  
 259 possible to identify cells and concave and convex  
 260 surfaces there.

$$225 \quad Y_i ((W \cdot X_i) + b) \geq 1$$

226  $\|W\|$  is the rule of a normal a numeric base and  
 227 (.)Specifies the number of production operation.  
 228 Using coefficient of Lagrangzhyan the value of  
 229 performance can be defined as follows:

261 Equation 1: general of curvature

$$230 \quad L = \frac{1}{2} \|W\|^2 - \sum_{i=1}^n \lambda_i (y_i ((w \cdot x_i) + b) - 1)$$

231  $\lambda_i$  is a Lagrangzhyan coefficient. This solution can  
 232 be calculated through minimization of binary  
 233 equation 3. Variation of variables bles B & W took  
 234 place in standard valuation methods:

$$262 \quad Z = Ax^2y^2 + Bx^2y + Cxy^2+Dx^2+Ey^2+Fxy+Gx+Hy+I$$

235

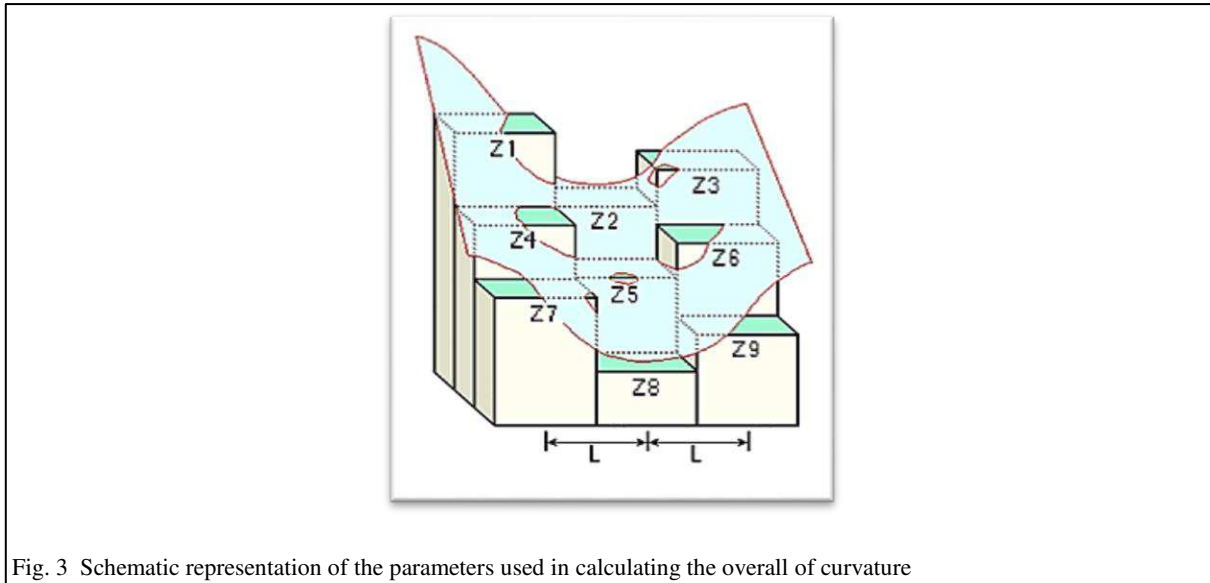


Fig. 3 Schematic representation of the parameters used in calculating the overall of curvature

263

264

265 Among a wide variety of curvatures, profile and  
 266 plan of curvature can be noted as two  
 267 geomorphometric index. The curvatures of the  
 268 profile represent the degree of change in profile  
 269 curvature along the way and therefore represent the  
 270 intensity of water flow and sedimentation  
 271 processes. So that the negative level of this  
 272 curvature shows convex surfaces and the positive  
 273 level shows concave surfaces (Pike., 2000).

274 Equation 2-2: the curvature profile.

$$275 \quad n * g * (a * d^2 + b * e^2 + c * d * e) / (d^2 + e^2) (1 + (d^2 + e^2))^{1.5}$$

276 On the other hand the curvature of the plan  
 277 represents a shift in direction through a curve, and  
 278 therefore represents a topographical divergence and  
 279 convergence. Negative values of the curvature of  
 280 the plan indicates the current divergence, which  
 281 includes the ridges and peaks and positive values  
 282 (valleys) show (Goudie., 1990) current  
 283 convergence. It is noteworthy that flat surfaces  
 284 have a curvature of zero. The curvature is measured  
 285 in radians or in meter (up to 100 m).

286 Equation 3: the curvature Plans

$$287 \quad n * g * (b * d^2 + a * e^2 - c * d * e) / (d^2 + e^2)^{1.5}$$

288 In all these relationships g: resolution of digital  
 289 elevation model, n: the dimensions of the moving  
 290 window.

### 291 Discussion and Results

292 Map of the existing landslides and the training  
 293 samples

294 In this study, to determine landslide susceptibility,  
 295 features of 39 landslides which had occurred in the  
 296 study area were taken using satellite images (PAN)  
 297 IRS and geographic information systems (GIS)  
 298 were analyzed. Samples which were randomly  
 299 collected from the landslide area were divided into  
 300 two groups: first those are used for model  
 301 production training and the examples which were  
 302 used in model validating tests (Marjanovi'c et al.,  
 303 2011). The main purpose of separating training and  
 304 testing of samples was building a model and  
 305 modeling test obtained by independent test  
 306 samples. When the randomly collected samples for  
 307 simultaneous training and testing are used with  
 308 random samples based on the pixel slip spots, the  
 309 model performance can be artificially increased  
 310 (Taner San., 2014).

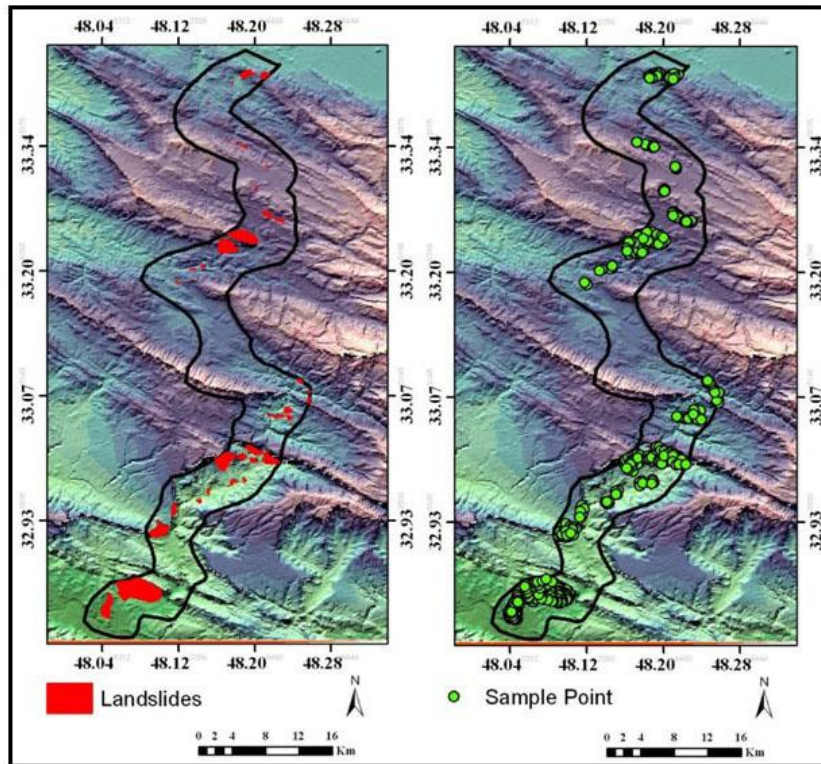


Fig. 4 Distribution of landslides and training samples in the study area

311

312

313 **zoning the landslide using the controller**  
 314 **parameters**

315 All effective and landslide controller variables  
 316 which are used as input in SVM model are shown  
 317 as a map (Figure 5) and a table (1):

318 **Direction range**

319 Direction of range is taken from of the DEM layer  
 320 and is defined as the frequency of slopedirections  
 321 of surface complications aspects. Accordingly,  
 322 ranges are classified in 9 levels as completely  
 323 smooth, North, North East, East, South East, South,  
 324 South-West, West and North West sorted (Figure  
 325 5).

326 **slope degree**

327 Slopes degree and its convexity, concavity and its  
 328 being direct has a large impact on landslide  
 329 occurrence. Because of the slope geometry, a  
 330 convex topographic surface is less steep (Lulseged  
 331 et al,2004). Steep slope increases the shear stress  
 332 caused by gravity and disrupts the range further  
 333 (Dai et al., 2001). As one of the most important  
 334 factors in instability, slope, was extracted from  
 335 hypsometric layer (Figure 5).

336 **land use**

337 Freeway construction and excavation and  
 338 embankment operations together with the

339 destruction of oak forests and meadows, without  
 340 any attention to principles of sustainability are  
 341 among the most important factors which stimulate  
 342 the dominant ranges over roads. In order to provide  
 343 an efficient map using Landsat TM images were  
 344 used and the general area was divided into four in  
 345 which the categories of agricultural lands and  
 346 gardens, meadows, forests and rocky surfaces.

347 **Distance from drainage**

348 Landslides on the sidelines of most of the  
 349 waterways in the area, especially around the main  
 350 river beds of Zal and Chameshk lead to instability  
 351 of dominant ranges. For this purpose, six floors  
 352 from long distances to those close to the waterways  
 353 and rivers in Figure 5 are provided to determine the  
 354 impact of these variables in case a landslide occurs  
 355 (Figure 5)

356 **Distance from the fault**

357 In the region, either directly (the energy of the  
 358 fault) and indirectly (the effect of lithology and  
 359 slope) landslides are caused by faults. To  
 360 understand the impact of this parameter buffers  
 361 were made from a distance of 5 Kilometers to the  
 362 active fault line, in the form of five stories as <5,  
 363 5-10, 10-15, 15-20,> 20 km (Figure 5).

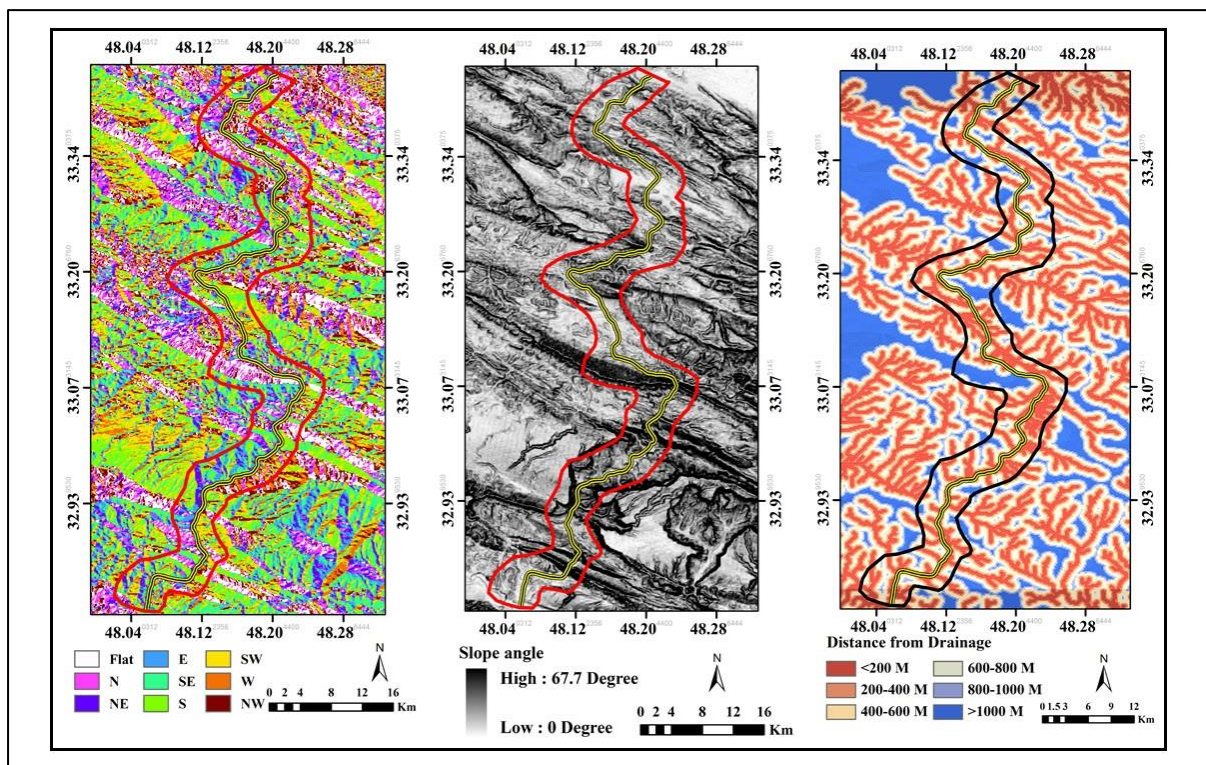
364 **Lithology**

365 Lithology is known as a key factor in creating 368 rocks in Fig. 4 and the descriptions of each of them  
 366 landslide in the form of erosion and weathering 369 is given in Table 1.  
 367 (Anbalagan, 1992 Dai et al., 2001). Distribution of  
 370

371 Table1 Geological units and their descriptions in the study area

Describing lithology	Geological units	The row number
Calcareous sandstone and silty marl with streaks column	MuPlaj	1
The cement conglomerate with limestone and marl	Plbk	2
Semi-hard conglomerate recent	Qc2	3
Dolomitic limestone, marl and clay with layers	EMass-Sb	4
Siltstone, sandstone, limestone marl	KPeam	5
Conglomerate sandstone and siltstone with interlayers	Ekn	6
Gypsum and clay marl with anhydrite	Mlgs	7
Marl and shale clay with traces of lime	Kgu	8
Shale and marl with limestone clay	Pb	9
Songs full of fossils	Tz – E - zang	10
Marl clay limestone with shale layers	Kbgp	11
Alluvium and debris recent	Qt2	12

372



373

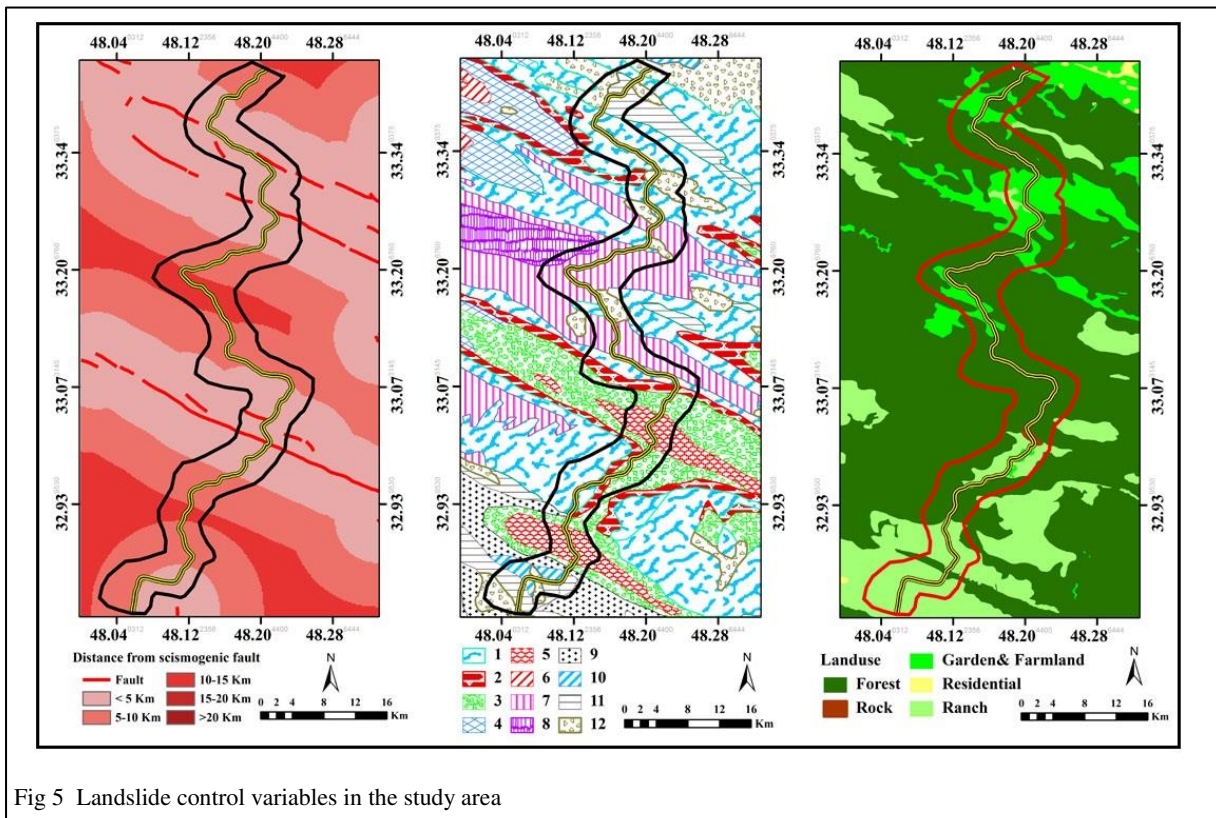
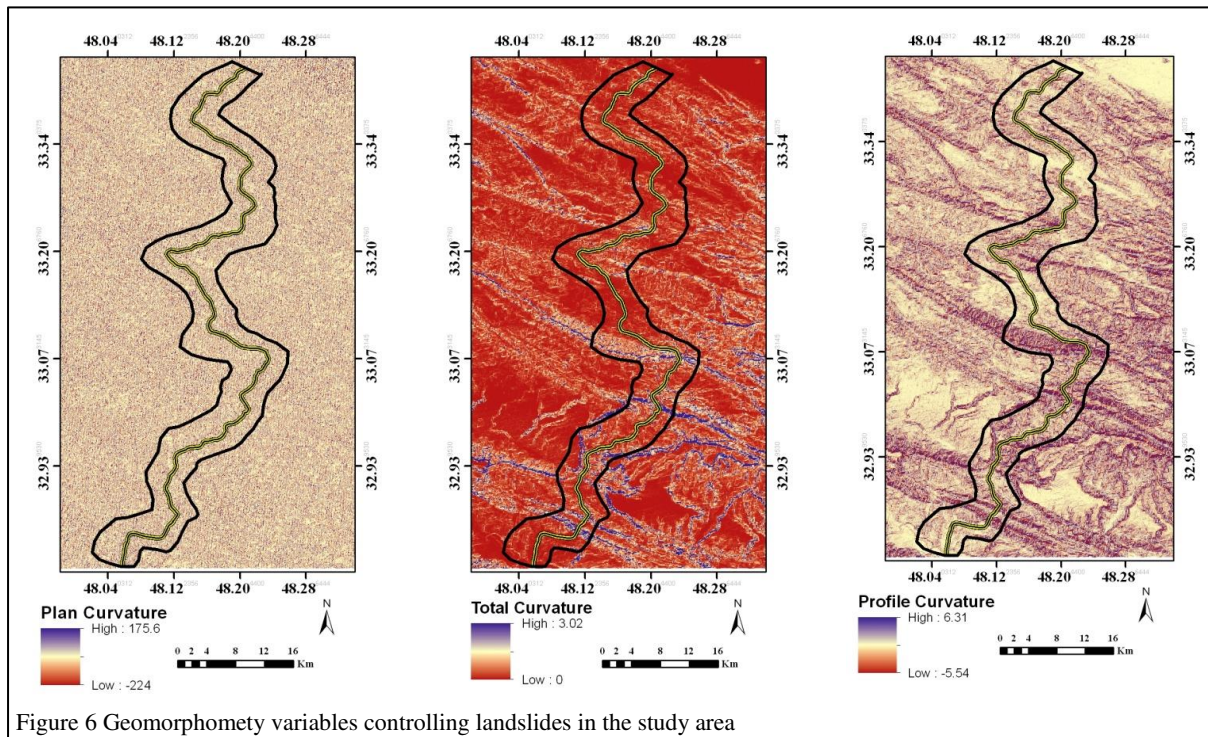


Fig 5 Landslide control variables in the study area

376 **Geomorphometric variables**

377 Rippling type of domains has a significant effect on  
 378 the occurrence of landslides. In most studies to  
 379 express rippling effect on the domain movement,  
 380 slope factor cannot show all the features of uneven  
 381 surface by itself. Therefore, in this study the  
 382 Geomorphometric variables of profile curvature,  
 383 and plan and the overall curvature which are  
 384 derivatives of second grade were used for  
 385 expressing roughness of the domain surface and  
 386 their effect on landslides and an attempt has been  
 387 made to use them for identifying areas prone to  
 388 landslides and thus model them more accurately  
 389 (Figure 6). The curve of the profile represents the

390 amount of change in profile curvature along the  
 391 way and therefore represents the intensity of water  
 392 flow and sedimentation and transportation  
 393 processes. Thus the amounts of negative curvature  
 394 show convex surfaces and concave surfaces are  
 395 shown by a positive amount. On the other hand, the  
 396 curvature of the plan represents a shift in direction  
 397 of the curve, and therefore represents a  
 398 topographical divergence and convergence.  
 399 Negative values of the curvature of the plan show  
 400 the current divergence, which includes the ridges  
 401 and peaks and positive values show flow  
 402 convergence (valleys). The overall curvature  
 403 specifies the overall shifts in the surface.



404 Figure 6 Geomorphometry variables controlling landslides in the study area

405 Using effective metrics on slip and  
 406 Geomorphometric indicators and using polynomial  
 407 and linear functions in SVM model, landslide prone  
 408 zones modeling was obtained in the study area,  
 409 which is done with regard to local modeling in the  
 410 ENVI software and model outputs are specified in  
 411 the form of a map (Figure 7). Maps of polynomial  
 412 and linear functions show zones which are sensitive  
 413 to landslide in Khorramabad - Paul zal highway.  
 414 Sensitivity values were between 0 and 1, and as we

415 got closer to 1 (Light Color on the map) aptness  
 416 and sensitivity for landslides in the study area  
 417 increases. The results show that more than 30  
 418 percent of the area under study, is located in areas  
 419 with more than 0.8 which indicates that the high  
 420 sensitivity of the study area of the slip. One reason  
 421 to the high sensitivity of the area is the passage of  
 422 the highway and cutting off the range and finally a  
 423 loss of balance in the region.

424

425  
426

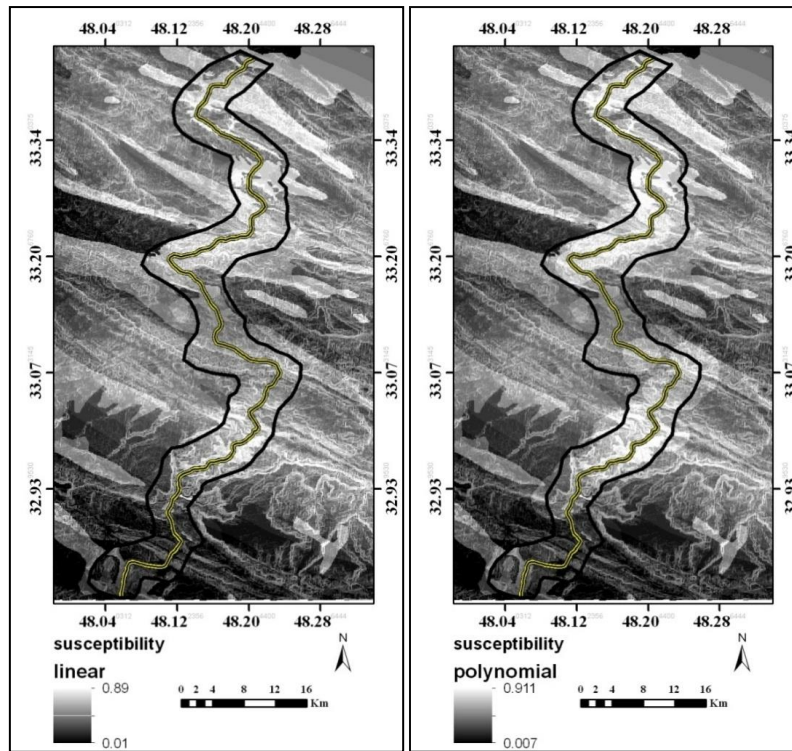


Figure 7 landslide susceptibility based on linear and polynomial function and SVM model in the study area

#### 427 assessment of accuracy of slip zoning 428 modeling

429 After application of each model, it is necessary to  
430 evaluate the accuracy to take action regarding the  
431 applicability and reality of results. In this study,  
432 twenty percent of the samples were used to assess  
433 accuracy carefully. First, an error matrix was  
434 formed and then using the overall accuracy,  
435 accuracy of the model was determined. The results  
436 show modeling through by polynomial function  
437 (polynomial) with an overall accuracy of 89% was  
438 more accurate and had a better performance and is  
439 more consistent with ground realities in comparison  
440 to the linear method with an overall accuracy of  
441 84%. Given that the behavior of the slip control  
442 variables in the study area has not been linear and  
443 has a non-linear complex behavior, Polynomial  
444 method has had a better modeling capability and  
445 mapping results are more compatible with the  
446 ground reality.

#### 447 Conclusion

448 Geomorphometry is the quantitative analysis of the  
449 shapes on the surface of the Earth and land surface  
450 conditions which carries out the quantitative  
451 analysis of uneven surfaces. In this study, the  
452 aforementioned indicators along with other  
453 variables have been used, in order to identify more

454 precisely uneven surfaces and their effects on the  
455 slip and eventually increase the accuracy of  
456 modeling. The results showed that the use of  
457 polynomial functions and linear SVM model in  
458 zoning the the area under study with the  
459 involvement of Geomorphometric factors of the  
460 domains has well identified the points with high  
461 landslide potential. Also evaluating the accuracy of  
462 the modeling showed that polynomial functions  
463 with the overall accuracy of 89% have shown the  
464 areas prone to landslide better than that the linear  
465 function which seems to be due to the complex and  
466 nonlinear behavior of the variables which are  
467 involved in landslide occurrences.

#### 468 References

- 469 -Akgun, A., Sezer, E.A., Nefeslioglu, H.A., Gokceoglu, C., Pradhan,  
470 B., 2012. An easy-to-use MATLAB program (MamLand) for the  
471 assessment of landslide susceptibility using a Mamdani fuzzy  
472 algorithm. *Computers & Geosciences*, 38, 23–34.  
473 doi:10.1016/j.cageo.2011.04.012  
474 -Anbalagan, R., 1992. Landslide hazard evaluation and zonation  
475 mapping in mountainous terrain. *Engineering Geology*, 32, 269–277.  
476 doi:10.1016/0013-7952(92)90053-2  
477 - Bui, D., Pradhan, B., Lofman, O., Revhaug, I., Dick, O., 2012.  
478 Landslide susceptibility mapping at Hoa Binh province (Vietnam)  
479 using an adaptive neuro fuzzy inference system and GIS. *Computers  
480 and Geosciences*. 45.199–211. doi:10.1016/j.cageo.2011.10.031  
481 - Chung, C., Fabbri, A., 2003. Validation of spatial prediction  
482 models for landslide hazard mapping. *Natural Hazards*, 30, 451–472.  
483 doi: 10.1023/B:NHAZ.0000007172.62651.2b  
484 - Dai, F.C., Lee, C.F., Li, J., Xu, Z.W., 2001. Assessment of  
485 landslide susceptibility on the natural terrain of Lantau Island, Hong  
486 Kong. *Environmental Geology*, 40, 381–391. doi:  
487 10.1007/s002540000163

488 -Ercanoglu, M., Gokceoglu, C., 2004. Use of fuzzy relations to  
489 produce landslide susceptibility map of a landslide prone area (West  
490 Black Sea Region, Turkey). *Engineering Geology*, 75, 229–250.  
491 doi:10.1016/j.enggeo.2004.06.001  
492 - Fell, R., Corominas, J., Bonnard, C., Cascini, L., Leroi, E., Savage,  
493 W., 2008. Guidelines for landslide susceptibility, hazard and risk  
494 zoning for land-use planning. *Engineering Geology*, 102, 99–111.  
495 doi:10.1016/j.enggeo.2008.03.014  
496 -Fisher, P., Wood, J., Cheng, T., 2004. Where is Helvellyn?  
497 Fuzziness of Multiscale Landscape Morphometry. *Transactions of  
498 the Institute of British Geographers*, 29 (1), 106–128.  
499 DOI: 10.1111/j.0020-2754.2004.00117.x  
500 -Frattini, P., Crosta, G., Carrara, A., 2010. Techniques for evaluating  
501 the performance of landslide susceptibility models. *Engineering  
502 Geology*, 111, 62–72. doi:10.1016/j.enggeo.2009.12.004  
503 - Guzzetti, F., Reichenbach, P., Ardizzone, F., Cardinali, M., Galli,  
504 M., 2006. Estimating the quality of landslide susceptibility models.  
505 *Geomorphology*, 81, 166–184. doi:10.1016/j.geomorph.2006.04.007  
506 - Lee, S., Ryu, J., Won, J., Park, H., 2004. Determination and  
507 application of the weights for landslide susceptibility mapping using  
508 an artificial neural network. *Engineering Geology*, 71, 289–302.  
509 doi:10.1016/S0013-7952(03)00142-X  
510 - Ling Peng, A.B., Ruiqing Niu, A., Bo Huang, C., Xueling Wu, A.,  
511 Yannan Zhao, A., Runqing Ye, D., 2014. Landslide susceptibility  
512 mapping based on rough set theory and support vector machines: A  
513 case of the Three Gorges area, China. *Geomorphology*, 204, 287–  
514 301. doi:10.1016/j.geomorph.2013.08.013  
515 -Lulseged, A., Yamagishi, H., Ugawa, N., 2004. Landslide  
516 susceptibility mapping using GIS-based weighted linear  
517 combination, the case in Tsugawa area of Agano river. *Niigata  
518 Prefecture, Japan, Landslide*, 1, 73– 81. Doi: 10.1007/s10346-003-  
519 0006-9  
520 -Nadim, F., Kjekstad, O., Peduzzi, P., Herold, C., Jaedicke, C., 2006.  
521 Global landslide and avalanche hotspots. *Landslides*, 3, 159–173.  
522 Doi:10.1007/s10346-006-0036-1  
523 -Nefeslioglu, H.A., Gokceoglu, C., Sonmez, H., 2008. An  
524 assessment on the use of logistic regression and artificial neural  
525 networks with different sampling strategies for the preparation of  
526 landslide susceptibility maps. *Engineering Geology*, 97, 171–191.  
527 doi:10.1016/j.enggeo.2008.01.004  
528 -Nefeslioglu, H.A., Sezer, E., Gokceoglu, C., Bozkir, A.S., Duman,  
529 T.Y., 2010. Assessment of landslide susceptibility by decision trees  
530 in the metropolitan area of Istanbul, Turkey. *Mathematical Problems  
531 in Engineering*, 1–15. doi:10.1155/2010/901095  
532 - Oh, H.-J., Pradhan, B., 2011. Application of a neuro-fuzzy model  
533 to landslide-susceptibility mapping for shallow landslides in a  
534 tropical hilly area. *Computers & Geosciences*, 37, 1264–1276.  
535 doi:10.1016/j.cageo.2010.10.012  
536 - Pike, R.J., 2000. Geomorphology - Diversity in quantitative surface  
537 analysis. *Progress in Physical Geography*, 24, 1–20.  
538 doi: 10.1177/030913330002400101  
539 -Pourghasemi, H.R., Mohammady, M., Pradhan, B., 2012. Landslide  
540 susceptibility mapping using index of entropy and conditional  
541 probability models in GIS: Safarood Basin, Iran. *Catena*, 97, 71–84.  
542 doi:10.1016/j.catena.2012.05.005  
543 - Pradhan, B., 2013. A comparative study on the predictive ability of  
544 the decision tree, support vector machine and neuro-fuzzy models in  
545 landslide susceptibility mapping using GIS. *Computers &  
546 Geosciences*, 51, 350–365. doi:10.1016/j.cageo.2012.08.023  
547 - Pradhan, B., Lee, S., Buchroithner, M., 2009. Use of geospatial  
548 data for the development of fuzzy algebraic operators to landslide  
549 hazard mapping: a case study in Malaysia. *Applied Geomatics*, 1, 3–  
550 15. DOI 10.1007/s12518-009-0001-5  
551 - Saito, H., Nakayama, D., Matsuyama, H., 2009. Comparison of  
552 landslide susceptibility based on a decision-tree model and actual  
553 landslide occurrence: the Akaishi Mountains, Japan. *Geomorphology*,  
554 109, 108–121. doi:10.1016/j.geomorph.2009.02.026  
555 - Talbot, C.J., Alavi, M., 1996. The past of a future syntax across  
556 the Zagros. *Geological Society, London, Special Publications*, 100,  
557 89 – 109. Doi: 10.1144/GSL.SP.1996.100.01.08  
558 -Talebi, A., Troch, P. A., Uijlenhoet, R., 2008. A steady state  
559 analytical slope stability model for complex hillslope. *Hydrological  
560 Processes*, 22, 546–553. DOI: 10.1002/hyp.6881  
561 -Taner San, B., 2014. An evaluation of SVM using polygon-based  
562 random sampling in landslide susceptibility mapping: The Candir  
563 catchment area (western Antalya, Turkey). *International Journal of  
564 Applied Earth Observation and Geoinformation*, 26, 399–412.  
565 doi:10.1016/j.jag.2013.09.010  
566 -Vapnik, V., 1995. *The Nature of Statistical Learning Theory*.  
567 Springer-Verlag, Inc., New York.  
568 - Wan, S., 2009. A spatial decision support system for extracting the  
569 core factors and thresholds for landslide susceptibility map.  
570 *Engineering Geology*, 108, 237–251.  
571 doi:10.1016/j.enggeo.2009.06.014  
572 - Wood, J., 1996. Scale-based characterization of digital elevation  
573 models. In: Parker, D. *Innovations in GIS*, Taylor and Francis,  
574 London, 163–175.  
575 -Yalcin, A., 2008. GIS-based landslide susceptibility mapping using  
576 analytical hierarchy process and bivariate statistics in Ardesen  
577 (Turkey): comparisons of results and confirmations. *Catena*, 72, 1–  
578 12. doi:10.1016/j.catena.2007.01.003  
579 - Yamani, M., Ahmadabadi, A., Zare, G.R., 2013. Application of  
580 support vector machine algorithm in landslide hazard zoning (Case  
581 study: Darake of watershed). *Geography and Environmental  
582 Hazards*, 3, 125–142.  
583 <https://www.sid.ir/en/journal/ViewPaper.aspx?id=295973>  
584 - Yamani, M., Shamsipour, A.A., Gourabi, A., Rahmati, M., 2014.  
585 Determining landslide zones in Khorramabad – Pole Zaal freeway  
586 by using Hierarchical Analysis – Fuzzy Logic method. *Applied  
587 Research of Geographic Sciences*, 32, 27–44.  
588 <https://www.sid.ir/en/journal/ViewPaper.aspx?id=403580>  
589 - Yamani, M., Shamsipour, Rahmati, M., 2014. The bounding of the  
590 present and quaternary zones of climate and morphogenesis  
591 processes in Khorramabad - Pole Zaal freeway. *Quantitative  
592 Geomorphological Researches*, 2, 90 – 103.  
593 [http://www.geomorphologyjournal.ir/article\\_77953.html](http://www.geomorphologyjournal.ir/article_77953.html)  
594 - Yao, X., Tham, L.G., Dai, F.C., 2008. Landslide susceptibility  
595 mapping based on support vector machine: a case study on natural  
596 slopes of Hong Kong, China. *Geomorphology*, 101, 572–582.  
597 doi:10.1016/j.geomorph.2008.02.011  
598 -Yeon, Y.K., Han, J-G., Ryu, K.H., 2010. Landslide susceptibility  
599 mapping in Injae, Korea, using a decision tree. *Engineering Geology*,  
600 116, 274–283. doi:10.1016/j.enggeo.2010.09.009  
601 -Yesilnacar, E., Topal, T., 2005. Landslide susceptibility mapping: a  
602 comparison of logistic regression and neural networks methods in a  
603 medium scale study, Hendek region (Turkey). *Engineering Geology*,  
604 79, 251–266. doi:10.1016/j.enggeo.2005.02.002  
605 -Yilmaz, I., 2009. Landslide susceptibility mapping using frequency  
606 ratio, logistic regression, artificial neural networks and their  
607 comparison: a case study from Kat landslides (Tokat, Turkey).  
608 *Computers & Geosciences*, 35, 1125–1138.  
609 doi:10.1016/j.cageo.2008.08.007  
610 -Marjanović, M., Kovačević, M., Bajat, B., Voženilek, V., 2011.  
611 Landslide susceptibility assessment using SVM machine learning  
612 algorithm. *Engineering Geology*, 123 (3), 225–234.  
613 doi:10.1016/j.enggeo.2011.09.006  
614 - Talebi, A., Uijlenhoet, R., Troch, P., 2008. A low dimensional  
615 physical based model of hydrologic control of shallow landsliding  
616 on complex hill slopes. *Earth Surf. Process. Landforms*, 33, 1964–  
617 1976. DOI: 10.1002/esp.1648  
618 - Xu, C., Dai, F., Xu, X., Lee, Y.H., 2012. GIS-based support vector  
619 machine modeling of earthquake-triggered landslide susceptibility in  
620 the Jianjiang River watershed, China. *Geomorphology*, 145–146,  
621 70–80. doi:10.1016/j.geomorph.2011.12.040

# Figures

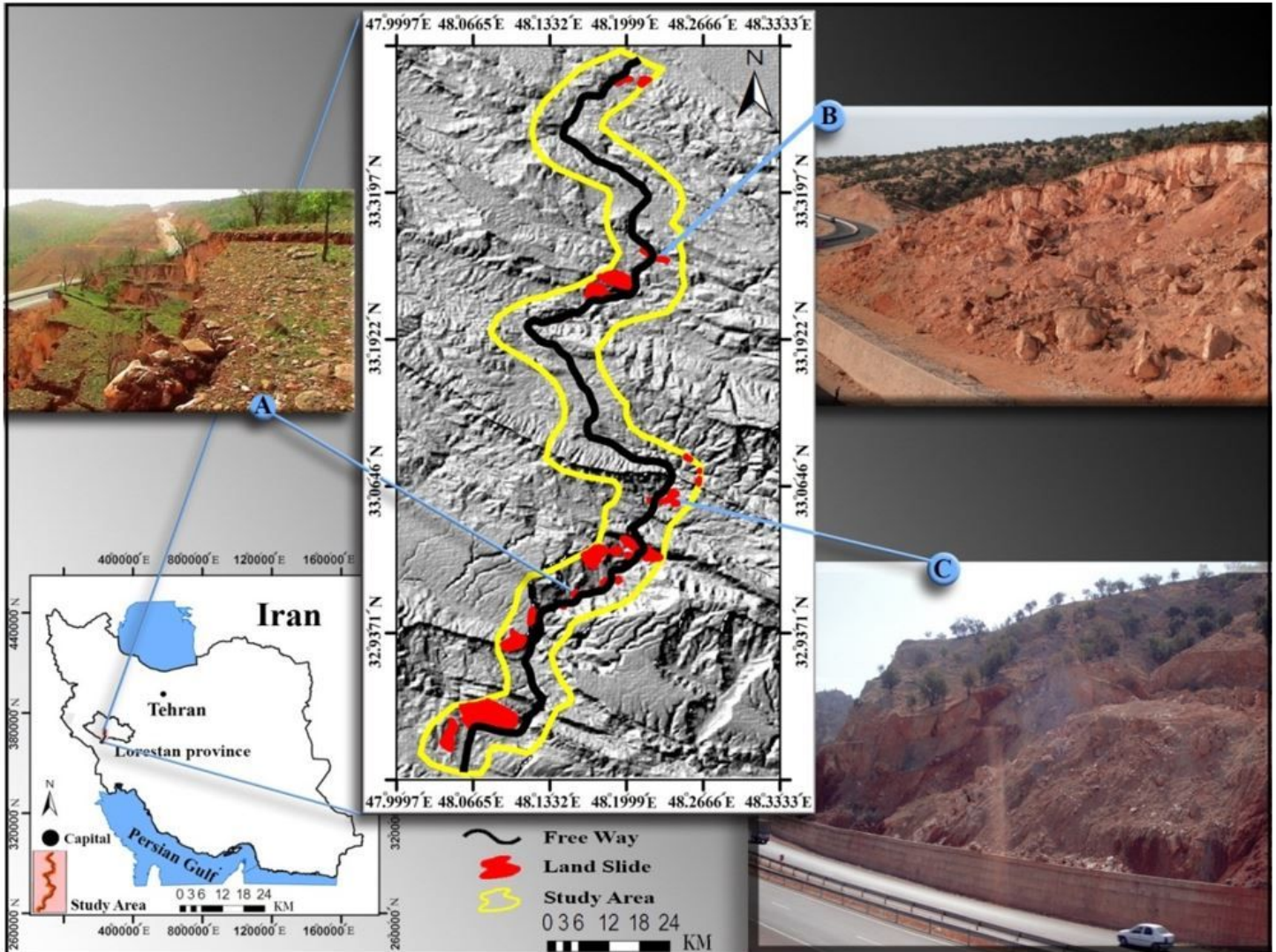


Figure 1

Location map of the area in Lorestan province and dispersion of sliding.

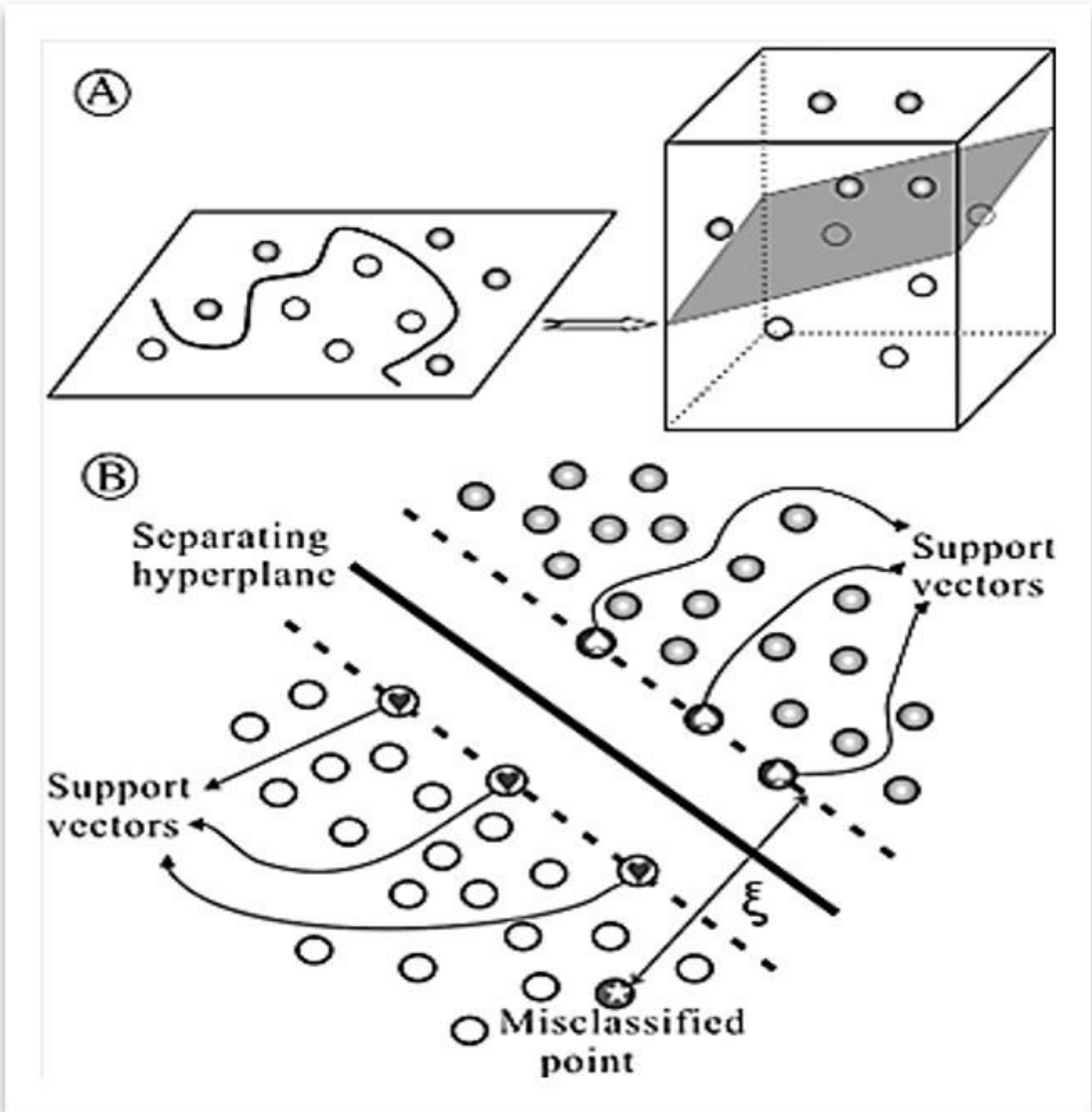


Figure 2

Image of the principles of SVM(A) n-dimensional Page differences between the two classes with a maximum distance(B) The inseparable and imprecise variables.

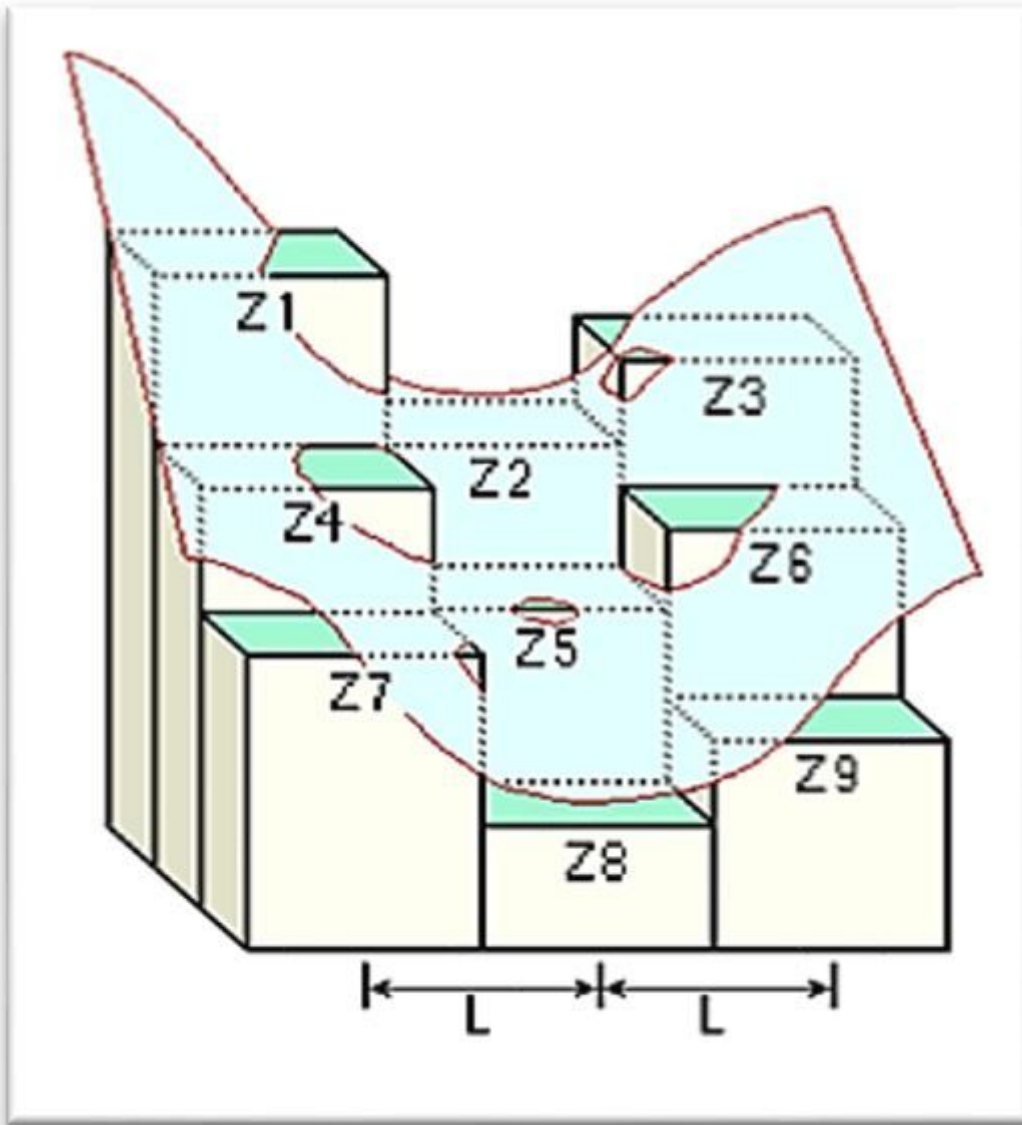


Figure 3

Schematic representation of the parameters used in calculating the overall of curvature.

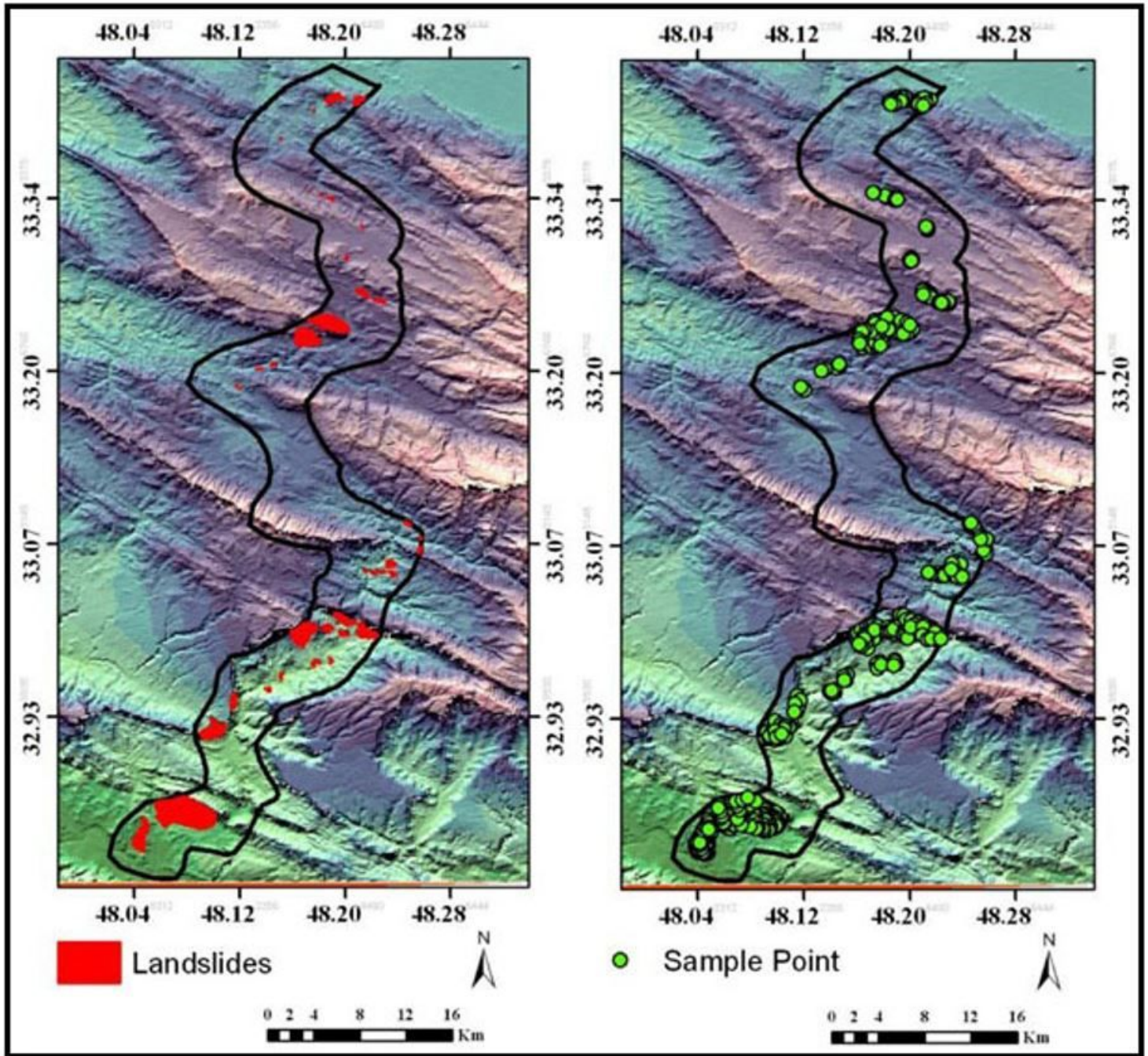


Figure 4

Distribution of landslides and training samples in the study area.

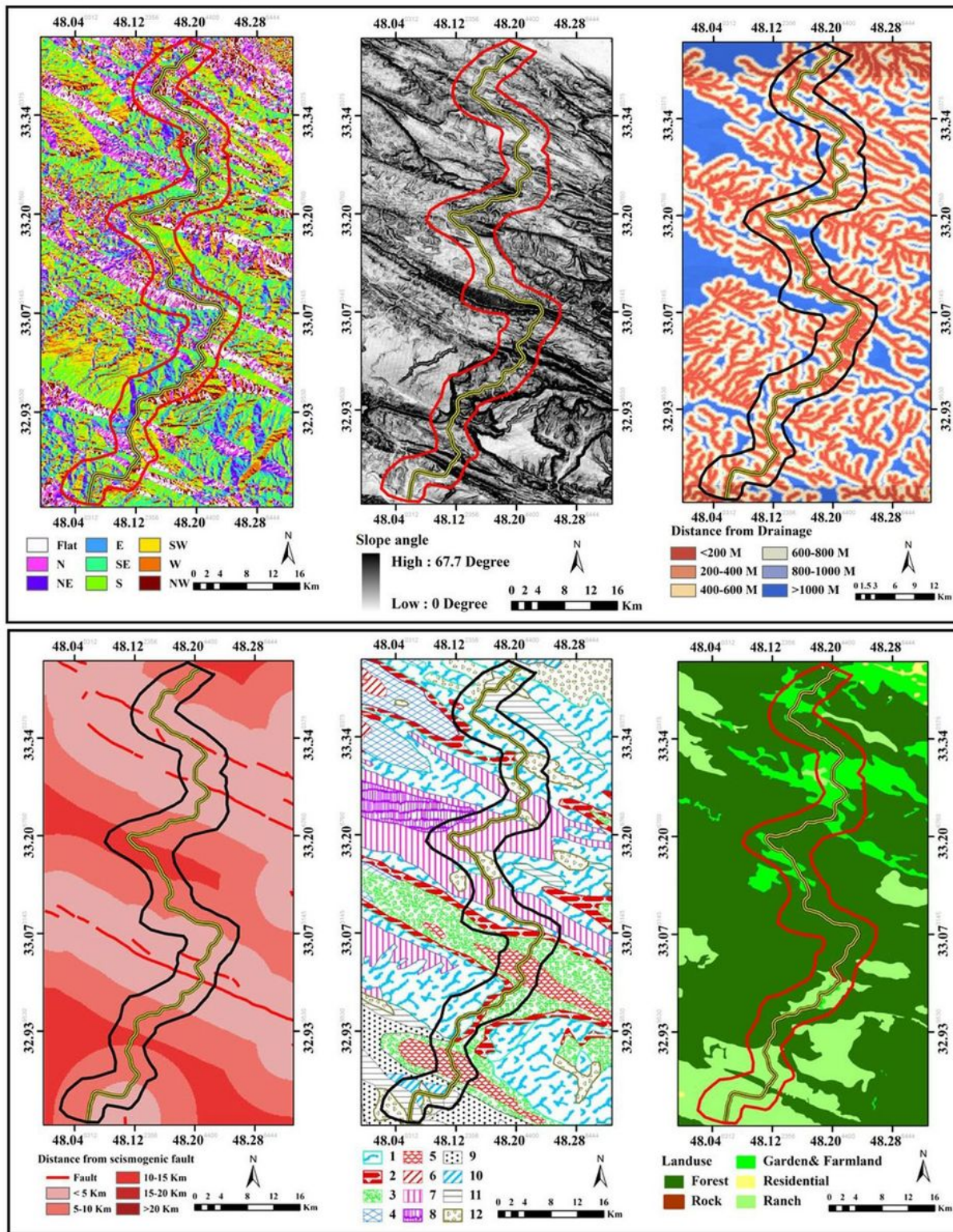
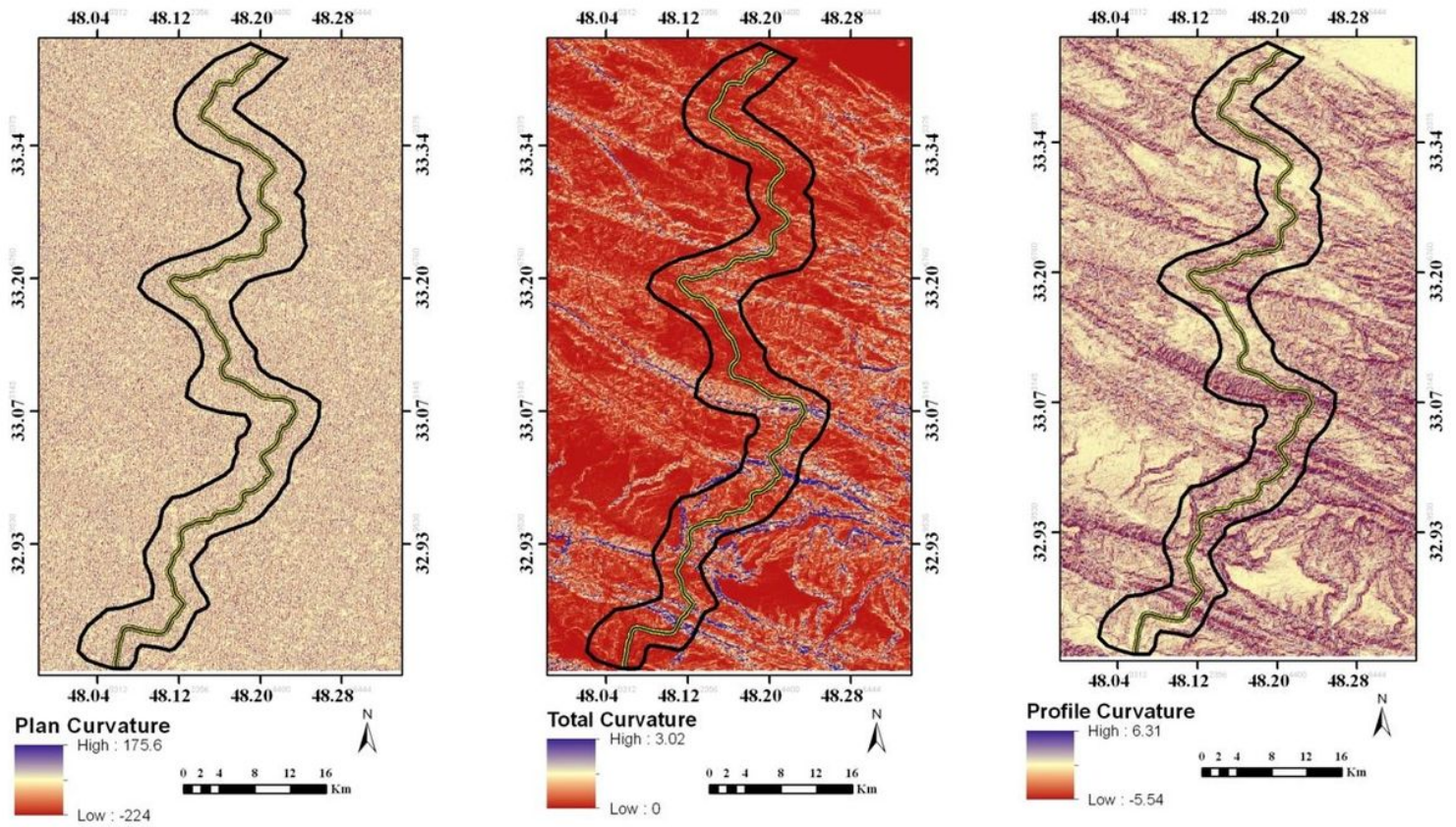


Figure 5

Landslide control variables in the study area.



**Figure 6**

Geomorphometry variables controlling landslides in the study area.

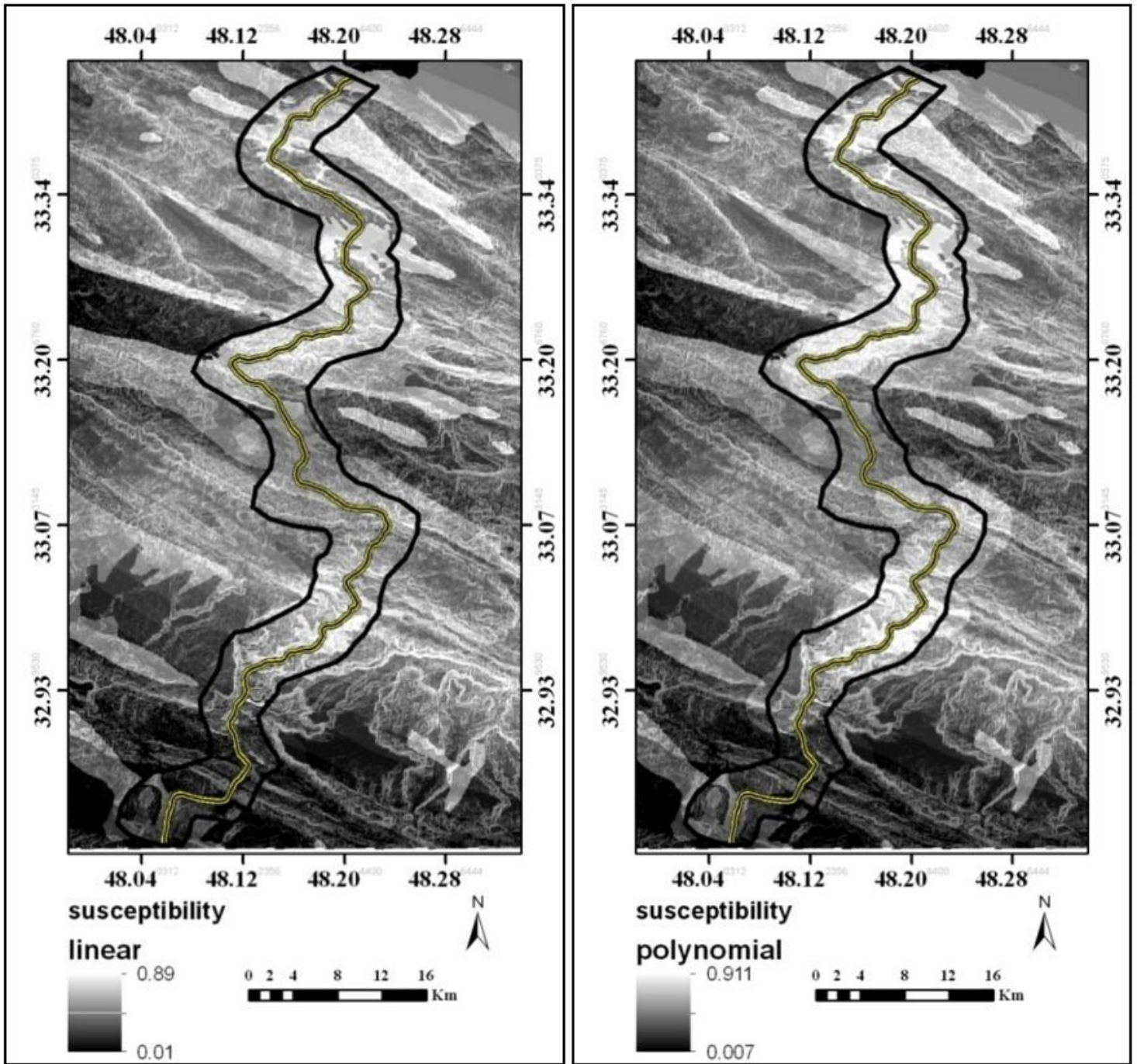


Figure 7

landslide susceptibility based on linear and polynomial function and SVM model in the study area.